NUCLEAR SCIENCE AND TECHNIQUES **26**, 040602 (2015)

Analysis and optimization of energy resolution of neutron-TPC*

HUANG Meng (黄孟),[1,2] LI Yu-Lan (李玉兰),[1,2,†] NIU Li-Bo (牛莉博),[1,2] LI Jin (李金),[1,2,3] and LI Yuan-Jing (李元景)[1,2]

[1]*Department of Engineering Physics, Tsinghua University, Beijing 100084, China*
[2]*Key Laboratory of Particle & Radiation Imaging (Tsinghua University), Ministry of Education, Beijing 100084, China*
[3]*Institute of High Energy Physics, Beijing 100049, China*

(Received August 27, 2014; accepted in revised form September 17, 2014; published online August 20, 2015)

Neutron-TPC (nTPC) is a fast neutron spectrometer based on GEM-TPC (Gas Electron Multiplier-Time Projection Chamber) and expected to be used in nuclear physics, nuclear reactor operation monitoring, and thermonuclear fusion plasma diagnostics. By measuring the recoiled proton energy and slopes of the proton tracks, the incident neutron energy can be deduced. It has higher n/γ separation ability and higher detection efficiency than conventional neutron spectrometers. In this paper, neutron energy resolution of nTPC is studied using the analytical method. It is found that the neutron energy resolution is determined by 1) the proton energy resolution ($\sigma_{E\mathrm{p}}/E_\mathrm{p}$), and 2) standard deviation of slopes of the proton tracks caused by multiple Coulomb scattering ($\sigma_{k(\mathrm{scattering})}$) and by the track fitting accuracy ($\sigma_{k(\mathrm{fit})}$). Suggestions are made for optimizing energy resolution of nTPC. Proper choices of the cut parameters of reconstructed proton scattering angles (θ_{cut}), the number of fitting track points (N), and the working gas help to improve the neutron energy resolution.

Keywords: Neutron-TPC, Energy resolution, Analytical method, Multiple Coulomb scattering

DOI: 10.13538/j.1001-8042/nst.26.040602

I. INTRODUCTION

Neutron-TPC (nTPC) is a fast neutron spectrometer under research, and is expected to be used in the fields of nuclear physics, nuclear reactor operation monitoring, and thermonuclear fusion plasma diagnostics [1–3]. It is based on a GEM-TPC (Gas Electron Multiplier-Time Projection Chamber) using argon and hydrocarbon mixture as the working gas at 1 atm [4, 5]. A field-cage made of polyimide and copper is installed between the cathode and readout board to establish an effective volume, and a triple-GEM module works as the electron multiplier. A collimated neutron beam entering into the sensitive volume will scatter with protons of the working gas (Fig. 1). By measuring the energy deposited by the scattered protons (E_p) in the sensitive volume and the slopes of proton tracks (k), one can deduce the incident neutron energy by Eq. (1).

$$E_\mathrm{n} = E_\mathrm{p}/\cos^2\theta = E_\mathrm{p}(1+\tan^2\theta) = E_\mathrm{p}(1+1/k^2), \quad (1)$$

where θ is the proton scattering angle, and $k = \tan(\theta + \pi/2) = -1/\tan\theta$.

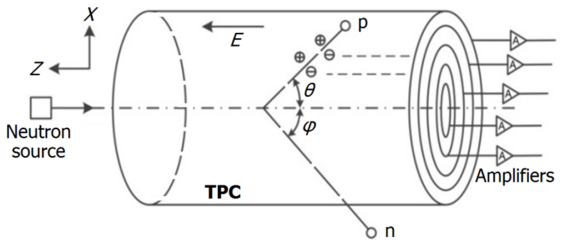

Fig. 1. Scheme of a neutron-TPC.

Thanks to TPC's ability of 3D-track reconstruction and its large gaseous volume, neutron-TPC is advantageous in its higher n/γ separation ability and detection efficiency than those of conventional neutron spectrometers, like the proton telescope system [2, 3, 6, 7]. By simulation based on the Geant4 software, neutron-TPC can reach a detection efficiency of ~0.1% and neutron energy resolution (FWHM) of better than 5% [1].

In this paper, we focus on deduction of analytical expressions of the neutron energy resolution of neutron-TPC, and discuss the optimization of neutron energy resolution based on simulations using Geant4 and Garfield [8–10]. Influences of different parameters on neutron energy resolution are studied quantitatively, which helps optimizing the detector structure and experimental parameters. Analytical expressions of the neutron-TPC's energy resolution are deducted, and methods to improve neutron energy resolution are suggested.

II. ANALYTICAL EXPRESSIONS

A. nTPC energy resolution

From Eq. (1), the neutron energy resolution ($\sigma_{E_\mathrm{n}}/E_\mathrm{n}$) can be derived by the resolutions of the proton energy ($\sigma_{E\mathrm{p}}/E_\mathrm{p}$) and the slope of proton track (σ_k/k).

$$\begin{aligned}\left(\frac{\sigma_{E_\mathrm{n}}}{E_\mathrm{n}}\right)^2 &= \left(\frac{\sigma_{E_\mathrm{p}}}{E_\mathrm{p}}\right)^2 + \left[\frac{\sigma_{\left(1+\frac{1}{k^2}\right)}}{1+\frac{1}{k^2}}\right]^2 \\ &= \left(\frac{\sigma_{E_\mathrm{p}}}{E_\mathrm{p}}\right)^2 + \left(\frac{-2\frac{1}{k^3}\cdot\sigma_k}{1+\frac{1}{k^2}}\right)^2 \\ &= \left(\frac{\sigma_{E_\mathrm{p}}}{E_\mathrm{p}}\right)^2 + \left(\frac{-2\sigma_k}{k^3+k}\right)^2.\end{aligned} \quad (2)$$

Assuming the incident neutrons are mono-energetic and only the protons with a certain scattering angle (θ) are studied in

* Supported by the National Natural Science Foundation of China (No. 11275109)
† Corresponding author, yulanli@mail.tsinghua.edu.cn

the data processing, then $E_{\rm p}$ is determined and the main task to improve the neutron energy resolution is to reduce standard deviations of the proton energy ($\sigma_{E_{\rm p}}$) and the slope of the proton track (σ_k).

In the data processing, $E_{\rm p}$ is deduced by the number of electrons collected by the readout pads. As a result, the standard deviation of the deduced proton energy ($\sigma_{E_{\rm p}}$) is mainly caused by the statistical fluctuation in the ionization process and the gain fluctuation of the GEM module. The slope k is deduced from the track reconstruction on the r-z plane. Two factors contribute to the slope uncertainty of the reconstructed proton track (σ_k): one is the multiple Coulomb scattering of protons ($\sigma_{\theta(\rm scattering)}$), another is the track fitting accuracy on the r-z plane ($\sigma_{k(\rm fit)}$). Therefore, the neutron energy resolution expression is the sum of three terms.

$$\left(\frac{\sigma_{E_{\rm n}}}{E_{\rm n}}\right)^2=\left(\frac{\sigma_{E_{\rm p}}}{E_{\rm p}}\right)^2+\left(\frac{-2\sigma_{k(\rm scattering)}}{k^3+k}\right)^2+\left(\frac{-2\sigma_{k(\rm fit)}}{k^3+k}\right)^2. \tag{3}$$

In the following paragraphs, detailed analysis will be put on these three terms.

B. Energy resolution of scattered protons

First, assume there is no electron attachment in the working gas and ignore the ADC (Analog-to-Digital Conversion) process. Then the proton energy deposited in the detector can be represented by electrons collected by the readout pads. Considering that the collected electrons come from two independent processes of the drift and avalanche, the number of electrons can be expressed as

$$n_A=n\cdot A, \tag{4}$$

where n is the primary electrons ionized by the protons, and A is the amplification factor of the GEM module. Therefore, the proton energy resolution equals the relative standard deviation of n_A

$$\begin{aligned}\left(\frac{\sigma_{E_{\rm p}}}{E_{\rm p}}\right)^2&=\left(\frac{\sigma_{n_A}}{n_A}\right)^2\\&=\left(\frac{\sigma_n}{\langle n\rangle}\right)^2+\frac{1}{\langle n\rangle}\cdot\frac{\sigma_A^2}{\langle A\rangle^2}\\&=\frac{1}{\langle n\rangle}\left(F+\frac{\sigma_A^2}{\langle A\rangle^2}\right)\\&=\frac{\bar{W}}{E_{\rm p}}\left(F+\frac{\sigma_A^2}{\langle A\rangle^2}\right)\\&=\frac{\bar{W}}{E_{\rm n}}\left(1+\frac{1}{k^2}\right)\left(F+\frac{\sigma_A^2}{\langle A\rangle^2}\right),\end{aligned} \tag{5}$$

where F is the Fano factor, which is 0.2–0.5 for gases, $\bar{W}$ is the average ionization energy, and $\sigma_A^2/\langle A\rangle^2$ is the relative variance of A, which represents the amplification feature of the GEM module. For the electron multipliers, the amplification factor obeys the Polya distribution [11],

$$A\sim P(A)=\frac{(1+\alpha)^{(1+\alpha)}}{\Gamma(1+\alpha)}\cdot\left(\frac{A}{\langle A\rangle}\right)^{\alpha}\cdot\exp\left[-(1+\alpha)\frac{A}{\langle A\rangle}\right], \tag{6}$$

where α is a free parameter determining the shape of distribution. The relative variance of the Polya distribution is given by $\sigma_A^2/\langle A\rangle^2=1/(1+\alpha)$, and $(\sigma_{E\rm p}/E_{\rm p})^2$ can be given by

$$\left(\frac{\sigma_{E_{\rm p}}}{E_{\rm p}}\right)^2=\frac{\bar{W}}{E_{\rm n}}\left(1+\frac{1}{k^2}\right)\left(F+\frac{1}{1+\alpha}\right). \tag{7}$$

From Eq. (5), one can find that, for a given neutron energy, the proton energy resolution decreases with the slope of proton track, while the scattering angle increases and the scattered proton energy decreases.

C. The σ_k(scattering)

In measuring proton tracks, the unavoidable multiple Coulomb scattering affects accuracy of the reconstructed proton scattering angle (θ). At small angles, the multiple scattering angle $\varphi_{\rm Coulumb}$ obeys the Gaussian distribution, while at large angles, it obeys the Rutherford scattering. Here, $\varphi_{\rm Coulumb}$ is defined as the angle between the initial direction of the recoiled proton and its final direction after a material of certain thickness. Based on the Highland Formula, one has the standard deviation of multiple scattering angles of incident ions in material [12]:

$$\varphi_{\rm Coulumb}=[13.6\,{\rm MeV}/(\beta pc)]\cdot z(l_0/X_0)^{1/2}[1+0.038\ln(l_0/X_0)], \tag{8}$$

where l_0 is the areal density of material, β is the velocity of the incident particle, p is the momentum of the particle, z is the atomic number of the particle, and c is the light velocity.

The radiation length of material, X_0, can be calculated by the empirical formula [12].

$$X_0 = 716.4A/[Z(Z+1)\ln(287Z^{-1/2})], \tag{9}$$

where A is the mass number of material, and Z is the atomic number of material. For a mixture or compound, the radiation length can be deduced by

$$\frac{1}{X_0} = \sum \frac{w_i}{X_i}, \tag{10}$$

where X_i is the radiation length of the i^{th} element and w_i is the corresponding fraction by weight.

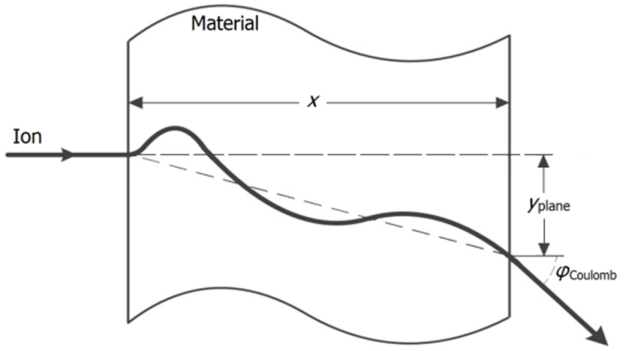

Fig. 2. Schematic diagram of multiple Coulomb scattering.

The standard deviation of proton recoil angles caused by multiple Coulomb scattering (Fig. 2) can be deduced [12].

$$\begin{aligned}\sigma_{\theta(\text{scattering})} &= \sigma_{y_{\text{plane}}}/x \\ &= \sigma_{\varphi_{\text{Coulomb}}} \cdot x \cdot 3^{-1/2}/x \\ &= 3^{-1/2}\sigma_{\varphi_{\text{Coulomb}}},\end{aligned} \tag{11}$$

where x is the thickness of the material, y_{plane} is the lateral displacement of particle through the material in the projection plane. The slope of proton track and the scattering angle is related by $k = -1/\tan\theta$, so $\sigma_{k(\text{scattering})}$ can be deduced from $\sigma_{\theta(\text{scattering})}$.

$$\begin{aligned}\sigma_{k(\text{scattering})} &= \sigma_{\theta(\text{scattering})}/\sin^2\theta \\ &= \sigma_{\theta(\text{scattering})}(1+k^2).\end{aligned} \tag{12}$$

To prove correctness of the analytical expressions of $\sigma_{k(\text{scattering})}$, a Monte Carlo simulation based on the Geant4 code was carried out. In the simulation, 1000 protons events were run for every parameter setting, and their final track positions were recorded to calculate $\sigma_{\theta(\text{scattering})}$. The results are given in Table 1. The Geant4 simulation results are just a little smaller than those from the analytical expressions. Therefore, the analytical method is consistent to estimate the standard deviation of the slope of the proton track caused by the multiple Coulomb scattering.

TABLE 1. Comparison of $\sigma_{\theta(\text{scattering})}$ from analytical expressions and Geant4 simulation

Gas	Thickness (cm)	E_p (MeV)	$\sigma_{\theta(\text{scattering})}$ (mrad)	
			Analytical	Simulation
Ar	5	3	19.6	17.1 ± 0.7
		5	11.8	9.8 ± 0.3
	10	3	28.8	27.2 ± 0.6
		5	17.3	15.5 ± 0.5
Ar-C_2H_6 (50 : 50)	5	3	15.6	13.7 ± 0.4
		5	9.4	7.7 ± 0.2
	10	3	22.9	21.7 ± 0.6
		5	13.8	11.7 ± 0.3

D. The $\sigma_{k(\text{fit})}$

Another factor resulting in the slope uncertainty of the reconstructed proton track is the accuracy of the track fitting process, which can be expressed as $\sigma_{k(\text{fit})}$ in the neutron-TPC, the projections of proton tracks on the r-z plane are approximately linear due to absence of magnetic field. Therefore, the fitting function of proton track points (r_i, z_i) is chosen as a linear function.

$$z = c_0 + c_1 r. \tag{13}$$

For different proton scattering angles, the slopes of fitting functions c_1 are also different. For a certain proton scattering angle, one can get the corresponding uncertainties of parameters c_0 and c_1 based on the Least Squares Method [13]:

$$\boldsymbol{V}_{\text{C}} = (\boldsymbol{F}^{\text{T}}\boldsymbol{W}_{\text{Y}}\boldsymbol{F})^{-1}, \tag{14}$$

where $\boldsymbol{V}_{\text{C}}$ is the covariance matrix of parameters c_0 and c_1.

$$\boldsymbol{V}_{\text{C}} = \begin{bmatrix} \sigma_{c_0}^2 & \text{cov}(c_0, c_1) \\ \text{cov}(c_1, c_0) & \sigma_{c_1}^2 \end{bmatrix}, \tag{15}$$

$$\boldsymbol{F} = \begin{bmatrix} 1 & r_1 \\ \vdots & \vdots \\ 1 & r_n \end{bmatrix}, \tag{16}$$

and $\boldsymbol{W}_{\text{Y}}$ is the weight matrix:

$$\boldsymbol{W}_{\text{Y}} = \begin{bmatrix} \sigma_{z_1}^2 & 0 & \cdots & 0 \\ 0 & \sigma_{z_2}^2 & \cdots & 0 \\ \cdots & \cdots & \cdots & \cdots \\ 0 & 0 & \cdots & \sigma_{z_N}^2 \end{bmatrix}^{-1}. \tag{17}$$

Standard deviation of the fitting parameter $c1$, which is just $\sigma_{k(\text{fit})}$, can be calculated by Eq. (18).

$$\begin{aligned}\sigma_{k(\text{fit})}^2 &= \sigma_{c_1}^2 \\ &= \frac{\sum_{i=1}^{N} \frac{1}{\sigma_{z_i}^2}}{\sum_{i=1}^{N} \frac{1}{\sigma_{z_i}^2} \cdot \sum_{i=1}^{N} \frac{r_i^2}{\sigma_{z_i}^2} - \sum_{i=1}^{N} \frac{r_i}{\sigma_{z_i}^2} \cdot \sum_{i=1}^{N} \frac{r_i}{\sigma_{z_i}^2}},\end{aligned} \tag{18}$$

where N is the number of points, r_i and z_i is the r- and z-coordinates of the fitting track point, and the σ_{z_i} is the z-resolution of neutron-TPC at $z = z_i$. Obviously, $\sigma_{k(\text{fit})}$ has a close relationship with N and σ_z, that is, $\sigma_{k(\text{fit})}$ decreases with increasing N or improving σ_z.

Next, the most important step is to parse the z-resolution of neutron-TPC σ_z. Generally, many factors will contribute to the z-resolution, including the intrinsic detector resolution, the gas properties, the tilt angle of the proton track with z-axis etc. Equation (19) can be obtained to represent the influences of factors on the z-resolution.

$$\sigma_z^2 = \sigma_{\text{detector}}^2 + \sigma_{\text{electronics}}^2 + \sigma_{\text{tilt\_angle}}^2 + \sigma_{\text{diffusion}}^2, \tag{19}$$

where σ_{detector} is the intrinsic detector resolution, which is related to the readout pads layout, the GEM module setting, uniformity of the drift electric field, etc.; $\sigma_{\text{electronics}}$ includes influences of electronic noise and analog-digital converting process; $\sigma_{\text{tilt\_angle}}$ is concerned with tilt angle of the proton track with z-axis, and can be expressed by Ref. [14].

$$\sigma_{\text{tilt\_angle}}^2 = d^2/(12\tan^2\theta N_{\text{eff}}), \tag{20}$$

where d is the pad width, θ is the tilt angle (also the proton scattering angle), and N_{eff} is the effective electron number; $\sigma_{\text{diffusion}}$ is caused by the longitudinal diffusion of electrons, and can be expressed by Ref. [4].

$$\sigma_{\text{diffusion}}^2 = D_{\text{L}}^2 z/N_{\text{eff}}, \tag{21}$$

where D_{L} is longitudinal diffusion coefficient of the working gas, z is the distance from the original position of ionized electrons to the readout board.

Based on Eq. (6), the effective electron number N_{eff} can be expressed as Eq. (22) [4].

$$N_{\text{eff}} = \frac{1}{\frac{\langle A^2\rangle}{\langle A\rangle^2}\cdot\langle\frac{1}{N}\rangle} = \frac{1}{\left(1+\frac{\sigma_A^2}{\langle A\rangle^2}\right)\cdot\langle\frac{1}{N}\rangle} = \frac{1}{\langle\frac{1}{n}\rangle}\left(\frac{1+\alpha}{2+\alpha}\right), \tag{22}$$

where A is the amplification factor of the GEM module, N is the number of drift electrons per pad row, and α is the parameter determining the shape of the Polya distribution. For $N \geq 50$, $\langle 1/N\rangle$ is close to $1/\langle N\rangle$, and N_{eff} can be given approximately by Eq. (23) [15].

$$N_{\text{eff}} \cong \langle N\rangle\left(\frac{1+\alpha}{2+\alpha}\right), \tag{23}$$

where $\langle N\rangle$ is the average number of drift electrons per pad row, and can be evaluated approximately based on the Bethe-Block formula [16].

$$\langle N\rangle \cong \frac{(-\mathrm{d}E/\mathrm{d}x)_{\text{ion}}\cdot d}{\sin\theta\cdot\bar{W}}, \tag{24}$$

$$(-\mathrm{d}E/\mathrm{d}x)_{\text{ion}} = \frac{z^2NZ}{v^2}\cdot\phi(v), \tag{25}$$

$$\phi(v) = \left(\frac{1}{4\pi\varepsilon_0}\right)^2 \cdot\frac{4\pi e^4}{m_0}\left[\ln\frac{2m_0v^2}{I} - \ln(1-(v/c)^2) - (v/c)^2\right], \tag{26}$$

where $-(\mathrm{d}E/\mathrm{d}x)_{\text{ion}}$ is the average energy loss per distance the protons traversing in the matter, d is the width of readout pads, θ is the recoil angle of protons, $\bar{W}$ is the average ionization energy, z is the proton charge, N is the density of the matter atoms, Z is the atomic number of the material, v is the velocity of protons, ε_0 is the vacuum permittivity, e is the electron charge, m_0 is the electron rest mass, $I = I_0Z$ is the mean excitation potential ($I_0 = 10\,\text{MeV}$), and c is the speed of light. Note that, the Bethe-Bloch formula is only suitable for the evaluation of the energy loss in material of charged particles with high energy (generally $> 1\,\text{MeV}$ for protons) [17, 18].

E. Evaluation of energy resolution of nTPC

Based on equations above, the energy resolution of neutron-TPC under specific parameters can be estimated. If the incident neutron energy E_{n} is 5 MeV, the recoiled protons are produced 50 cm away from the readout board with a scattering angle of 30°, and the working gas is Ar-C_2H_6 (50 : 50) at 1 atm, then the relative neutron energy resolution would be deduced as follows.

First, if $\alpha = 0.5$, $F = 0.2$, and $\bar{W} = 26\,\text{eV}$ (for Ar-C_2H_6 of $\sim$ 50 : 50), then the value of $(\sigma_{Ep}/E_{\text{p}})^2 = 6.01\times10^{-6}$. Second, if the number of fitting points is 20% of the number of track points, then $[-\sigma_{k(\text{scattering})}/(k^3+k)]^2 = 1.28\times10^{-4}$. Third, if the longitudinal diffusion coefficient D_{L} of electron is 231.4 μm/cm$^{1/2}$ (based on the Garfield simulation for the drift field of 200 V/cm), the pad width is 2 mm, and the z-resolution caused by σ_{detector} and $\sigma_{\text{electronics}}$ is 300 μm (based on experimental results), then $-(\mathrm{d}E/\mathrm{d}x)_{\text{ion}} = 12.4\,\text{MeV}$, $N_{\text{eff}} = 1.14\times10^3$, and $[-\sigma_{k(\text{fit})}/(k^3+k)]^2 = 4.62\times10^{-5}$. As a result, the neutron energy resolution $(\sigma_{E_{\text{n}}}/E_{\text{n}}) = 1.3\%$, corresponding to a FWHM of 3.2%. It means that, if all the protons are of recoil angles less than 30°, the neutron energy resolution (FWHM) will be better than 3.2%.

III. OPTIMIZATION OF NTPC ENERGY RESOLUTION

For certain incident neutron energy and proton scattering angle used in the neutron energy calculation, the nTPC energy resolution is dominated by three parameters: the proton energy resolution, standard deviations of t the proton track slope caused by multiple Coulomb scattering, and the accuracy of fitting procedure. In other words, the factors influencing the three parameters indirectly affect the reconstructed neutron energy resolution, such as the cut of reconstructed proton scattering angle θ_{cut}, the number of fitting track points, and choice of the working gas. Therefore, optimization of

the nTPC energy resolution will focus on discussing these factors. Besides, the neutron detection efficiency should be taken into account, which is of importance, too, for a neutron spectrometer.

A. Cut of reconstructed proton scattering angle ($\theta_{\rm cut}$)

As described in Section II A, for mono-energetic incident neutron beams, energy of the scattered protons increases, and the proton energy resolution improves, with decreasing proton scattering angle. Besides, a higher proton energy leads to a longer proton track, which helps improve accuracy of the reconstructed proton scattering angle. Therefore, setting a proper cut of reconstructed proton scattering angle will probably improve the neutron energy resolution. However, this will decrease the neutron detection efficiency. Considering distribution of the proton scattering angle cross-section (σ_θ) for fast neutron (<10 MeV) [19].

$$\sigma_\theta = (4\sigma_0 \sin^2\theta)/\pi \quad \theta \in [0, \pi/2], \tag{27}$$

where σ_0 is the total cross-section of proton scattering. The neutron detection efficiency (η) can be derived as

$$\begin{aligned}\eta &= \eta_0 \cdot \frac{\int_0^{\theta_{\rm cut}} \frac{4\sigma_0 \cdot \sin^2\theta}{\pi} \cdot {\rm d}\theta}{\sigma_0} \\ &= \eta_0 \cdot \frac{4}{\pi} \cdot \left[\frac{\theta_{\rm cut}}{2} - \frac{\sin(2\theta_{\rm cut})}{4}\right],\end{aligned} \tag{28}$$

where η_0 is the intrinsic neutron detection efficiency of neutron-TPC.

In order to demonstrate effects of the cutting angle method, a Monte Carlo simulation was carried out. The effective volume of neutron-TPC was based on a real TU-TPC (Φ300 mm $\times$ 500 mm); the working gas was Ar-C_2H_6 (50 : 50); the drift electric field was set as 200 V/cm; the ring-shaped readout pad was of 2 mm width; and the 5 MeV incident neutron beam was collimated along the z-axis. The number of fitting points (N) was 80% of the whole number of track points ($N_{\rm all}$). The parameters of working gas, such as electron drift velocity (3.89 cm/μs), and transverse and longitudinal diffusion coefficients of 293.3 and 231.4 μm/cm$^{1/2}$, respectively, were calculated by Garfield program. Proton recoil and ionization processes were simulated by the Geant4 code based on the physics list of QGSP_BIC_HP, and the energy deposition of recoiled protons in the effective volume was recorded [20]. Then, electron drift, diffusion and track reconstruction were simulated by ROOT code using the fast MC method [21].

The results are shown in Fig. 3, one finds that the neutron energy resolution improves, but detection efficiency deteriorates, with decreasing cutting angle ($\theta_{\rm cut}$). With the parameters set above, a neutron energy resolution (FWHM) of better than 5% and a detection efficiency of over 0.1% can be achieved at the cutting angle of 30°. Therefore, the essence of the cutting angle method is to compromise between the neutron energy resolution and the neutron detection efficiency.

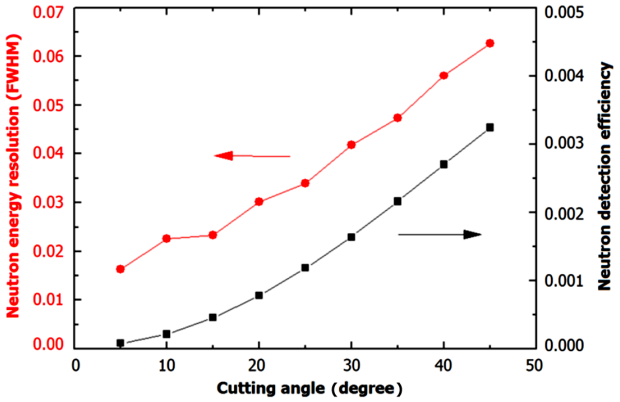

Fig. 3. (Color online) Neutron energy resolution and detection efficiency vs. cutting angle ($\theta_{\rm cut}$).

Note that, the simulation did not take into account the GEM module setting, the uniformity of drift field, electronics noise and the analog-to-digital conversion process, i.e. the parameters $\sigma_{\rm detector}$ and $\sigma_{\rm electronics}$ in Eq. (19) were not included in the simulation. Therefore, this simulation just provides an ideal result approximately, and further studies concerning $\sigma_{\rm detector}$ and $\sigma_{\rm electronics}$ will be carried out in the future.

B. Number of fitting track points

The number of fitting track points (N) affects standard deviation of the slope of reconstructed proton track. On one hand, N determines the multiple Coulomb scattering angle of the reconstructed proton track. The multiple Coulomb scattering angle and the standard deviation of the slope increase with N. On the other hand, from Eq. (18), the increase of N decreases uncertainty caused by the track fitting process. Therefore, there exists an optimal value N, which leads to the smallest standard deviation of the slope, and the best neutron energy resolution.

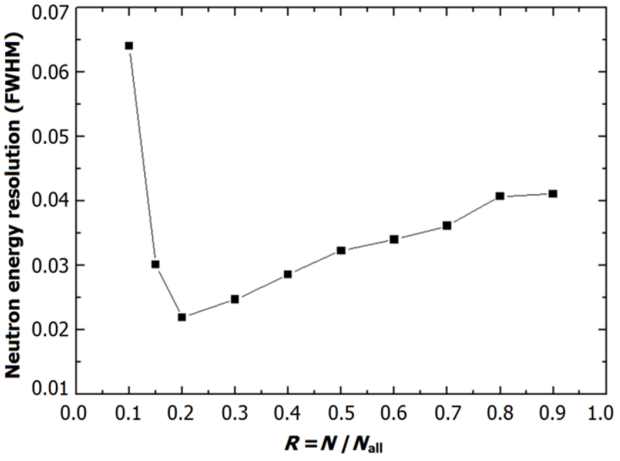

Fig. 4. Neutron energy resolution vs. number of fitting track points.

Take the simulation with the parameters the same as in Sec. III A, especially, $\theta_{\rm cut} = 30°$. Considering the differences of proton track lengths at different recoil angles, a new variable R is defined as the ratio of the number of fitting points (N) and the whole number of track points ($N_{\rm all}$). As shown in Fig. 4, at $R = 0.2$, the neutron energy resolution (FWHM) is the smallest ($\sim$2.2%). So, in data processing of nTPC, an optimized N is of great importance.

C. Choice of the working gas

In nTPC, the working gas plays both roles of ionizing medium and neutron detection medium. Generally, there are some basic principles of choosing a working gas of nTPC: 1) being of large enough detection efficiency for fast neutrons; 2) ensuring proper operation of the GEM module; and 3) contributing to a good neutron energy resolution. This section will mainly discuss the influence of the working gas on the neutron energy resolution.

The characteristics of the working gas concerning the neutron energy resolution includes the transverse diffusion coefficient ($D_{\rm T}$), the longitudinal diffusion coefficient ($D_{\rm L}$), the track length of recoiled proton (L), and the multiple Coulomb scattering angle of protons ($\varphi_{\rm Coulumb}$). First, the transverse and longitudinal diffusion coefficients affect z-resolution of the nTPC, and small $D_{\rm T}$ and $D_{\rm L}$ help achieving a good resolution of the slope of reconstructed proton track. Next, a longer L a larger whole number of track points ($N_{\rm all}$), which influences in turn choice of the number of fitting track points (N) and accuracy of the track fitting process. Finally, a smaller standard deviation of $\sigma_{\varphi_{\rm Coulumb}}$ leads to a smaller deviation of the slope of the reconstructed proton track. As a whole, in order to reach a good neutron energy resolution, the working gas shall bear the following characteristics: small enough transverse and longitudinal diffusion coefficients, a proper proton track length, and a small enough standard deviation of multiple Coulomb scattering angle of protons.

Based on the Bragg-Kleeman rule, the track length in material can be calculated by Ref. [16]

$$L_1/L_0 = \rho_0 A_1^{1/2}/(\rho_1 A_0^{1/2}), \tag{29}$$

where L is the track length, ρ is the density of the material, A is the atomic weight or effective atomic weight of the material, and the subscripts 1 and 0 denote the material studied and the air as reference, respectively. For compounds and complexes, the effective atomic weight ($A_{\rm eff}$) can be calculated by $A_{\rm eff}^{1/2} \cong \sum n_i A_i^{1/2}$, where n_i is the number fraction of the $i^{\rm th}$ atom. Therefore, the density (ρ) and atomic weight (or effective atomic weight) of the working gas determine the track length of protons in the drift chamber. So, a lower density and larger atomic weight (or effective atomic weight) leads to a longer proton track.

From Eq. (8), the areal density (l_0) and the atomic number (Z) of the material determine the multiple Coulomb scattering angle for the same incident ion. Considering l_0 is product of density and thickness of the material, when the material thickness is constant, the multiple scattering angle increase with the material density or the atomic number (Z). For the nTPC of constant N, the density (ρ) and the atomic number (Z) of the working gas determine the standard deviation of $\sigma_{\varphi_{\rm Coulumb}}$ of the reconstructed proton track.

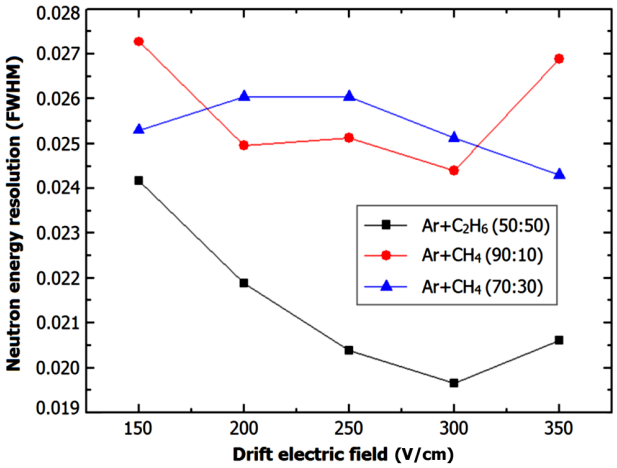

Fig. 5. (Color online) Neutron energy resolution as function of drift electric field, for the nTPC using different working gases.

Argon and hydrocarbon mixtures are used as working gases for nTPCs, such as Ar-CH_4 (90 : 10), Ar-CH_4 (70 : 30), and Ar-C_2H_6 (50 : 50). Figure 5 shows the Geant4 simulation results of energy resolution of the nTPC using the three gas mixtures, as function of the drift electric field ($E_{\rm drift}$). In the simulation, the ratio of number of fitting track points and the whole number of track points was $N/N_{\rm all} = 0.2$, and the cutting angle was $\theta_{\rm cut} = 30°$. Note that the simulation did not take into account the electric noise and ADC procedure, and the gas parameters in the different drift fields, such as electron drift velocity and diffusion coefficients, were calculated based on the Garfield simulation. From Fig. 5, at $E_{\rm drift} = 300$ V/cm, the neutron energy resolution of Ar-C_2H_6 (50 : 50) reaches minimum for its relatively low transverse and longitudinal diffusion coefficient. With its relatively high hydrogen content, Ar-C_2H_6 (50 : 50) is a good alternative as the working gas of nTPC. Studies will be done with more working gases.

IV. CONCLUSION

This paper mainly focuses on deduction of analytical expressions of the neutron-TPC energy resolution. The neutron energy resolution ($\sigma_{E_{\rm n}}/E_{\rm n}$) can be influenced by three factors: the proton energy resolution ($\sigma_{E{\rm p}}/E_{\rm p}$), standard deviation of the slope of proton track caused by the multiple Coulomb scattering angle ($\sigma_{k({\rm scattering})}$) and by the fitting accuracy ($\sigma_{k({\rm fit})}$). Based on the analytical expressions, one can estimate the neutron-TPC's energy resolution under certain parameters, and optimize the resolution by proper choice of the cut of reconstructed proton scattering angle ($\theta_{\rm cut}$), the number of fitting track points (N), and the working gas. The

setting and analysis of θ_{cut} and N are performed in the data processing, which have no direct relationship with the detector's structure, while the choice of the working gas is the key factor concerning optimization of the detector's structure to improve its energy resolution. From the Geant4 simulation results, Ar-C_2H_6 $(50:50)$ is a good choice as the working gas of nTPC, with higher detection efficiency for fast neutron and a better neutron energy resolution than those of other gases.

[1] Huang M, Li Y L, Deng Z, *et al*. A fast neutron spectrometer based on GEM-TPC. IEEE Nuclear Science Symposium and Medical Imaging Conference (NSS/MIC), 2012, 146–148. DOI: 10.1109/NSSMIC.2012.6551080

[2] Mori C, Gotoh J, Uritani A, *et al*. High-energy resolution spectrometer with proportional counter and Si-detector telescope type for 14 MeV neutrons in plasma diagnostics. Nucl Instrum Meth A, 1999, **422**: 75–78. DOI: 10.1016/S0168-9002(98)01066-3

[3] Matsumoto T, Harano H, Uritani A, *et al*. Fast neutron spectrometer composed of position-sensitive proportional counters and Si(Li)-SSDs with excellent energy resolution and detection efficiency. IEEE Nucl Sci Conf R, 2004, **2**: 715–719. DOI: 10.1109/NSSMIC.2004.1462311

[4] Li Y L. The design, construction and experimental study of a GEM-TPC prototype. Ph.D. Thesis, Tsinghua University, 2007. (in Chinese)

[5] Sauli F. GEM: A new concept for electron amplification in gas detectors. Nucl Instrum Meth A, 1997, **386**: 53l–534. DOI: 10.1016/S0168-9002(96)01172-2

[6] Ji C S. Neutron Detection Experimental Methods, 1998.

[7] Hawkes H P, Bond D S, Croft S, *et al*. The design of a proton recoil telescope for 14 MeV neutron spectrometry. Nucl Instrum Meth A, 2002, **476**: 506–510. DOI: 10.1016/S0168-9002(01)01498-X

[8] Agostinelli S, Allison J, Amako K, *et al*. Geant4–a simulation toolkit. Nucl Instr Meth Phys Res A, 2003, **506**: 250–303. DOI: 10.1016/S0168-9002(03)01368-8

[9] Veenhof R. Garfield, recent developments. Nucl Instrum Meth A, 1998, **419**: 726–730. DOI: 10.1016/S0168-9002(98)00851-1

[10] Niu L B, Li Y L, Zhang L, *et al*. Performance simulation and structure design of Binode CdZnTe gamma-ray detector. Nucl Sci Tech, 2014, **25**: 010406. DOI: 10.13538/j.1001-8042/nst.25.010406

[11] Kobayashi M. An estimation of the effective number of electrons contributing to the coordinate measurement with a TPC. Nucl Instrum Meth A, 2006, **562**: 136–140. DOI: 10.1016/j.nima.2006.03.001

[12] Groom D E and Klein S R. Passage of particles through matter. Eur Phys J C, 2000, **15**: 163–173. DOI: 10.1007/BF02683419

[13] Li Y Q. Experimental data processing, Hefei (China): Press of USTC, 2003. (in Chinese)

[14] Kobayashi M, Yonamineb R, Tomioka T, *et al*. Cosmic ray tests of a GEM-based TPC prototype operated in Ar-CF4-isobutane gas mixtures: II. Nucl Instrum Meth A, 2014, **767**: 439–444. DOI: 10.1016/j.nima.2014.08.027

[15] Kobayashi M. An estimation of the effective number of electrons contributing to the coordinate measurement with a TPC: II, Nucl. Instrum. Meth A, 2013, **729**: 273–278. DOI: 10.1016/j.nima.2013.07.028

[16] Knoll G F. Radiation detection and measurement. 3rd (Ed). NewYork(USA): John Wiley & Sons, 1989.

[17] Paul H and Schinner A. Statistical analysis of stopping data for protons and alphas in compounds. Nucl Instrum Meth B, 2006, **249**: 1–5. DOI: 10.1016/j.nimb.2006.03.010

[18] Paul H and Schinner A. Judging the reliability of stopping power tables and programs for protons and alpha particles using statistical methods. Nucl Instrum Meth B, 2005, **227**: 461–470. DOI: 10.1016/j.nimb.2004.10.007

[19] Liu J L. Study on the neutron spectrum measurement method based on optical imaging. Beijing: Tsinghua University, 2013.

[20] Geant 4. Reference physics lists. http://geant4.cern.ch/support/proc_mod_catalog/physics_lists/referencePL.shtml

[21] ROOT. Data analysis framework. http://root.cern.ch/